Effect of diode size and series resistance on barrier height and ideality factor in nearly ideal Au/n type-GaAs micro Schottky contact diodes

M. A. Yeganeh[a)b)†], Sh. Rahmatallahpur[b)], A. Nozad[b)], and R. K. Mamedov[a)]

[a)] *Faculty of Physics, Baku State University, Academic Zahid Xəlilov Küçəsi–23, AZ 1148, Iran*
[b)] *Material Research School, POB* 55515196, *Binab, Iran*

(Received 31 March 2010; revised manuscript received 29 April 2010)

Small high-quality Au/n type-GaAs Schottky barrier diodes (SBDs) with low reverse leakage current are produced using lithography. Their effective barrier heights (BHs) and ideality factors from current–voltage (I–V) characteristics are measured by a Pico ampere meter and home-built I–V instrument. In spite of the identical preparation of the diodes there is a diode-to-diode variation in ideality factor and barrier height parameters. Measurement of topology of a surface of a thin metal film with atomic force microscope (AFM) shows that Au-n type-GaAS SD consists of a set of parallel-connected micro and nanocontacts diodes with sizes approximately in a range of 100–200 nm. Between barrier height and ideality factor there is an inversely proportional dependency. With the diameter of contact increasing from 5 μm up to 200 μm, the barrier height increases from 0.833 up to 0.933 eV and its ideality factor decreases from 1.11 down to 1.006. These dependencies show the reduction of the contribution of the peripheral current with the diameter of contact increasing. We find the effect of series resistance on barrier height and ideality factor.

Keywords: Schottky barrier diodes, conducting probe-atomic force microscope, barrier height and ideality factor

PACC: 7280E, 7340S

1. Introduction

Gallium arsenide (GaAs) is one of the most important semiconductors that has intrinsic electronic properties superior to silicon, such as a direct energy gap, higher electron mobility, high breakdown voltage, chemical inertness, mechanical stability and lower power dissipation. These advantages of GaAs make it attractive for optoelectronic devices, discrete microwave devices and large-scale integrated electronic devices. GaAs has been used as radiation detector materials. The major advantage of this material is its ability to work at room temperature.[1−9]

Rectifying metal-semiconductor (MS) contacts, i.e. Schottky diodes (SDs), are widely used in modern electronic devices and well defined by fundamental energy model of Schottky where according to a contact potential difference between the metal and semiconductor, the potential barrier is formed on interface.

Most important parameters for I–V characteristics in Schottky contact are ideality factor and barrier height. The ideality factor n can be found from its forward current–voltage (I–V) characteristics.[10−12] Following the suggestion of Song *et al.*[13] regarding the role of inhomogeneities in the interfacial oxide layer composition and thickness in developing of the barrier inhomogeneities, in the early 1990s, Tung *et al.*,[14−17] Werner *et al.*,[18] and Biber *et al.*,[19] mentioned that the barrier height (BH) is likely to be a function of the interface atomic structure and the atomic inhomogeneities at the MS interface which are caused by facets, defects, grain boundaries and mixture of different phases. Therefore, they suggested that non-ideal behaviour of the Schottky barrier diodes (SBDs) could be quantitatively explained by assuming a distribution of nanometer-scale interfacial patches of reduced Schottky barrier height (SBH). Monch *et al.*[20−22] experimentally proved that the linear relationship between effective BH and ideality factor can be explained by lateral inhomogeneities of the BH. It was only in the last decade that by considering the inhomogeneities of the MS interface these devices have attracted much attention and well progressed and played a crucial role in constructing some useful devices in electronic technology and used for technical deficiencies such as surface processing, clean room, vacuum preparation and deposition techniques to produce proper contacts.

†Corresponding author. E-mail: myeganeh@bnrc.ir

© 2010 Chinese Physical Society and IOP Publishing Ltd

Due to the expectation of significant deviation from conventional behaviour for nano-diodes, an increasing interest is devoted to the study of the effects of downscaling lateral dimension on the electrical behaviour of the MS contact and to the detection of the local SBH on the nanometer scale.[23−33]

In spite of identical preparation of the diodes there is a diode-to-diode variation in ideality factor and barrier height parameters. It is found that for the diodes with diameters smaller than 200 μm the diode barrier height and ideality factor dependency on their diameters and the correlation between the diode barrier height and its ideality factor are nonlinear, similar to the case for the different metal semiconductor diodes earlier reported in the literature where these parameters for the manufactured diodes with diameters more than 100 μm are also linear. Also we find that series resistance affects barrier height and ideality factor.

We prepare small Au/n-GaAs Schottky diodes and obtain current–voltage characteristics for small Au/n-GaAs Schottky diodes. We demonstrate the nonlinear dependencies of BH and ideality factor on the diode diameter, derive the correlation between the diode BH and its ideality factor and study the influence of the patches, i.e. the inhomogeneities, by reducing the diode size.

2. Experimental procedure

In this work an n-type GaAs with Sn impurity, crystal direction of (1 0 0), a thickness of 300 μm, and $N_{\rm A} = 6\times10^{16}/{\rm cm}^3$ was selected. The sample surfaces were polished, and for cleaning the standard method was applied. For ohmic contact pure aluminum with a resistivity of 2.7 nΩ-Cm was used. Deposition procedure was done immediately after cleaning in a vacuum chamber at about 6.7×10^{-3} Pa, pure aluminum was deposited to 200-nm thick, monitored by quartz crystals, and ratio of coating was 3 Å/s (1 Å = 0.1 nm), then samples were annealed in an oven with H_2 gas at 570 °C for 10 min. Schottky contacts were patterned by wet lithography. Prior to the gold evaporation, the patterned samples were dipped in H_2SO_4:H_2O (1:10) for 3 min to remove the native oxidations and then rinsed in DI water. The Schottky contacts were made by evaporating 300 nm of gold onto the sample at a rate of 1.5 Å/s in a vacuum better than 1.3×10^{-3} Pa at a substrate temperature of 25 °C.

3. *I–V* measurement

I–V measurements were performed at room temperature using a homebuilt *I–V* measuring unit composed of a Keithley 4586 and three-dimensional probe stations with a 40-nm diameter Pt–Ir probe. A total of 20 patterns were fabricated on a single wafer. Figure 1 shows the measured $\ln(I)$–V curves for forward and reverse biases from 5 to 200 μm patterns for one sample. After each measurement, the tip was lifted from the contact and then we re-established electrical contact for current stability.

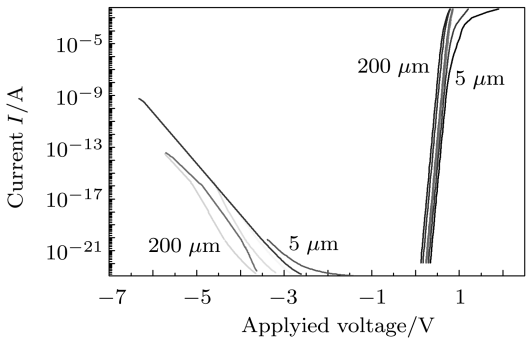


Fig. 1. Typical measured $\ln(I)$–V curves for forward bias (right) and reverse bias (left) from 5 to 200 μm patterns.

Figure 1 shows that the device exhibits a good rectification effect. From this figure we obtained the values of saturated current ($I_{\rm s}$) ranging from $I_{\rm s} = 1.4\times10^{-15}$ A to $I_{\rm s} = 3.37\times10^{-12}$ A.

4. Theory

Theoretical and experimental data for the values of work functions received by different methods, for simple substances of many chemical elements (polycrystalline and monocrystalline), chemical compounds (polycrystalline and monocrystalline) and firm solutions (polycrystalline and monocrystalline) are collected in Ref. [3]. Values of work functions both for simple substances, and all chemical compounds and firm solutions are basically in a range of 2–6 eV. At the same time it is firmly established that the sides of monocrystalline having various crystallographic orientations possess different values of work function. For a given substance, the work function of a side is larger than that on this side where atoms of a monocrystal are more densely located. The difference in work function depending on crystallographic orientation achieves nearby 1 eV. The image of a typical non-uniform emission surface of a metal electrode is schematically presented in Fig. 2(a). On this

surface along the ox axis, seven patches with local work functions Φ_{M1}, Φ_{M2}, Φ_{M3}, Φ_{M4}, Φ_{M5}, Φ_{M6}, Φ_{M7} (Fig. 2(b)) are displayed. Under the condition of $\Phi_{M1} > \Phi_{M2} < \Phi_{M3} > \Phi_{M4} < \Phi_{M5} > \Phi_{M6} < \Phi_{M7}$ variations of local work functions along the ox axis are presented in Fig. 2(c). It is clear that in each patch the local work function remains constant. It is clear that such a dependency of work function actually should not occur because the patches with different local surface work functions are in direct electric contact with surrounding patches. As a result a potential difference between surfaces of patches, so-called electrostatic spot field E_f,[3] is formed (Fig. 2(d)). The direction of the spot field is such that the spot field decelerates electrons emitted by the areas possessing smaller work functions but accelerates the electrons from the above areas with larger work functions. Consequently, the average work function Φ_{MS} remains constant along the ox axis (see a continuous line in Fig. 2(e)). In the presence of the spot fields, the work Φ done by an electron to escape from the Fermi level of emitter and move to infinity is unequal to local work functions of different parts of surface. In the absence of external electric field the total work Φ of the removal of electron is identical for all parts of surface and is determined by formula[3]

$$\bar{\Phi}_M = \frac{\int_s \Phi_M(s)\,ds}{A}, \quad \Phi_{MS} = \Phi_M - \Phi_S\ , \qquad (1)$$

where A is the surface area of the emitter, $\Phi_M(s)$ is the local work function in the individual surface and Φ_{MS} is the work function averaged over the total surface of diode. Local work function in the spot field is positive for the section where $\Phi_M < \Phi_S$, and negative for the section where $\Phi_M > \Phi_S$.

The spot fields on the patches with small local surface work functions ($\Phi_M < \Phi_{MS}$) are almost the same as an external restraining field between the flat electrodes and they reduce the current density emitted from these patches. On the contrary, they accelerate the electrons emitted from those patches with the local surface work function more than the average work function ($\Phi_M > \Phi_{MS}$). In close contact of metal with the monocrystalline semiconductor, the spot field penetrates into the semiconductor and actively participates in the formation of potential barrier and current transport.[3] To be specific, we examine the metal surface containing two types of patches with local surface work functions Φ_{M1} and Φ_{M2} where $\Phi_{M1} < \Phi_{M2}$ and they alternate regularly on the surface. The energy diagrams of patches with an n-type semiconductor of work function Φ_S before close contact are presented in Figs. 3(a) and 3(b) for the case where $\Phi_{M2} > \Phi_{M1} > \Phi_S$. By connecting the metal and the semiconductor by an electric wire with vacuum gap δ (Fig. 3(c)), Fermi levels of metal F_m and semiconductor F_s are aligned and between them there is a contact potential difference U_C (see the energy diagram presented in Fig. 3(d)). Electric field E_C of a contact potential difference between the metal and the semiconductor completely concentrates in vacuum gap δ between them. Thus, spot fields E_f on a surface of patches with Φ_{M1} are directed oppositely with respect to field E_C and spot fields on a surface of patches with Φ_{M2} are directed in parallel to the field E_c. Therefore the work function $\Delta\Phi_{M1}$ on surfaces of patches with Φ_{M1} will decrease with Φ_{M2} according to normal Schottky effect and it reduces $\Delta\Phi_{M2}$ in magnitude.

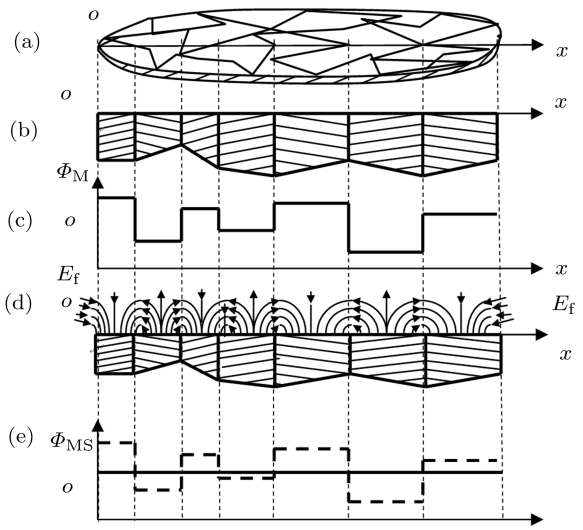


Fig. 2. Schematic diagrams of non-uniform surface (a), surfaces containing various micro crystals (b), various local work functions (c), local surface work functions along axis x and electric spot field E_f (d), and average work functions (e).

With reducing contact distance between metal and semiconductor and in the absence of a spot field, the layer of semiconductor is formed by static space charges of depletion layer with depth d_1 for patches with Φ_{M1} and depth d_2 for patches with Φ_{M2}, where $d_2 > d_1$. Actually, at close contact, a spot field may go so deep into the semiconductor that depth l_o is larger than d_1, i.e., $l_o > d_1$ (Fig. 3(e)), for patches with Φ_{M1}, under the influence of a spot field the depletion region layer goes deep and an additional potential barrier of $\Delta\Phi_{B1}$ is formed. For patches with Φ_{M2} the barrier height reduces $\Delta\Phi_{B2}$.

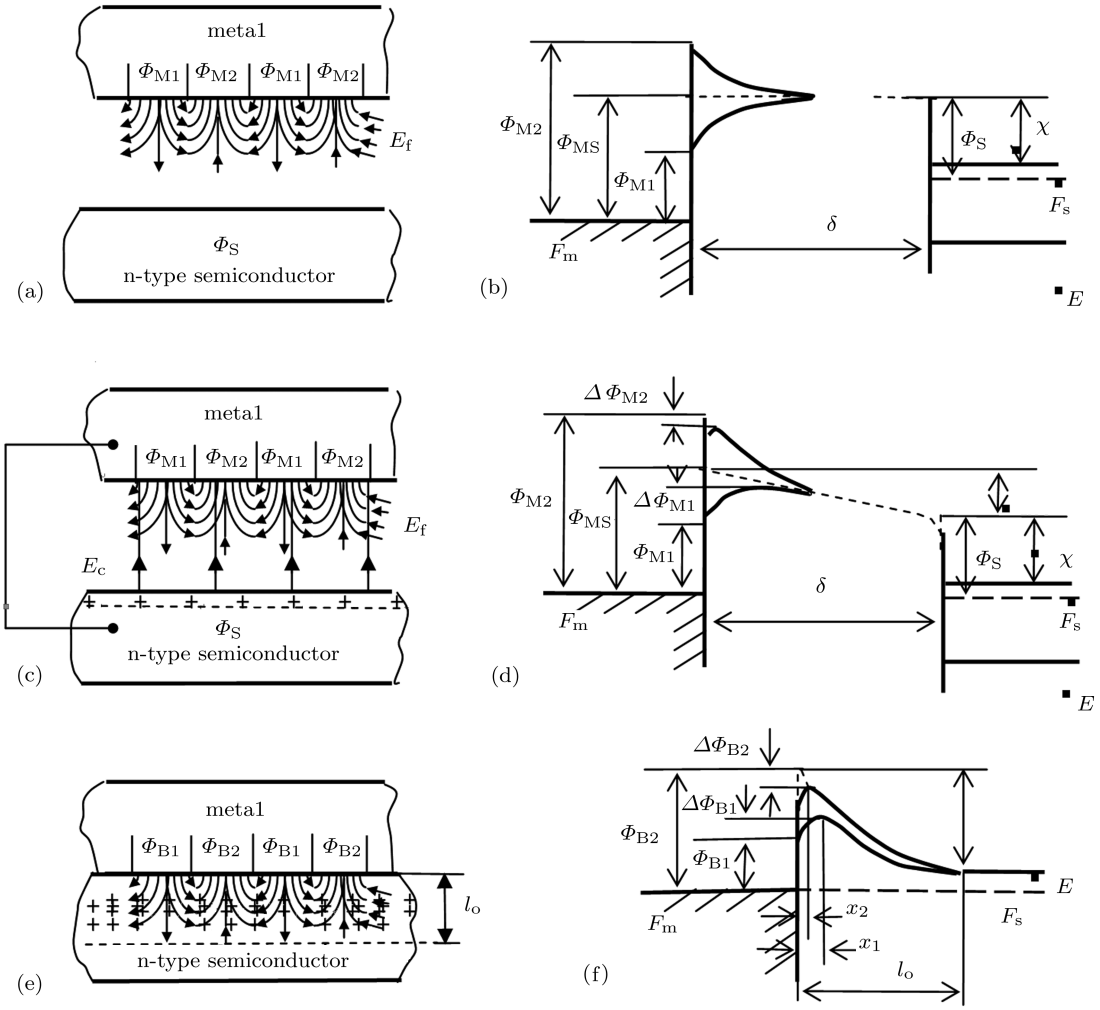


Fig. 3. Schematic structures and energy diagrams of the parallel-connected interacting rectifying contacts of metal with the n-type semiconductor in the presence of additional electric field.

Thus, as can be seen from Fig. 3(f), the barrier height of a patch with Φ_{B2} under the influence of both a contact potential difference and the spot field, reduces $\Delta\Phi_{B2}$ and becomes $\Phi_{B2} - \Delta\Phi_{B2}$, where its maximum is located at a distance (x_2) from surface of metal. And for a patch with Φ_{B1} under the influence of a spot field an additional barrier potential of $\Delta\Phi_{B1}$ is formed and the barrier height becomes $\Phi_{B1} + \Delta\Phi_{B1}$ with maximum located at a distance (x_2) from the surface of metal. Thus the distance x_1 for the patch with Φ_{B1} becomes much larger than the distance x_1 form the patch with Φ_{B2}.

In real metal–semiconductor (MS) contacts, patches with quite different configurations, various geometrical sizes and local work functions are randomly distributed on the surface of metal, hence direction and intensity of spot field are non-uniformly distributed along the surface of metal, and the formation of potential barrier is determined by the type of conductivity and the concentration of impurity in the semiconductor. According to Ref. [3], if real Schottky diode contains micro patches with the local potential barrier heights in an interval of $\Phi_{B\,min} - \Phi_{B\,max}$ then it is characterized by uniform operating height of potential barrier Φ_{BA} and characteristic distance x from a surface of metal. With designations $\Phi_{B\,min} = \Phi_{B1}$ and $\Phi_{B\,max} = \Phi_{B2}$, the operating height of a barrier depending on a degree of heterogeneous contact can be significant in an interval: $\Phi_{B1} + \Delta\Phi_{B1} \leq \Phi_{BA} \leq \Phi_{B2} - \Delta\Phi_{B2}$, and characteristic distance x is important in an interval $x_1 \leq x \leq x_2$, hence, the energy diagram of real Schottky diode in the absence of an external voltage is represented in Fig. 4 (dash line).

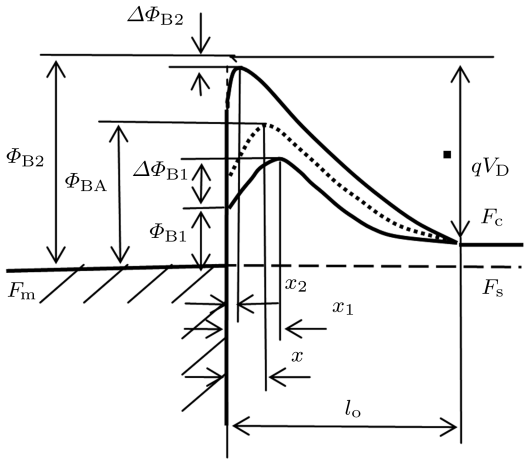


Fig. 4. Energy diagram of non-uniform Schottky diode in the absence of external voltage.

The current–voltage characteristic of real non-uniform Shottky diode is described by the following formula:[3]

$$\begin{aligned} I &= AA^*T^2 \exp\left(-\frac{\Phi_B}{kT}\right)\left[\exp\left(\frac{qV}{kT}\right)-1\right] \\ &= AA^*T^2 \exp\left(-\frac{\Phi_{BO}+\Delta\Phi_B}{kT}\right) \\ &\quad \times\left[\exp\left(\frac{qV}{kT}\right)-1\right], \end{aligned} \tag{2}$$

where V is the applied voltage, A the area of the diode, A^* Richardson's constant, T absolute temperature, k Boltzsman's constant, q electron charge, Φ_{BO} the operating local barrier height in the absence of an external voltage, $\Delta\Phi_B$ the additional potential barrier caused by both mirror image force and electric spot field.

The value of $\Delta\Phi_B$ is determined by the average value of barrier height Φ_{BS} over the contact area S where it is similar to the formula (1) and expressed as

$$\Phi_{BS} = \frac{\int_s \Phi_{BO}(s)\,\mathrm{d}s}{A}. \tag{3}$$

When $\Phi_{BO} > \Phi_{BS}$, the value of $\Delta\Phi_B$ is determined by the following formula:

$$\Delta\Phi_B = -q\left[\frac{q^3 N_D}{8\pi^2\varepsilon_s^3}\left(V_D \pm V - \frac{kT}{q}\right)\right]^{1/4}, \tag{4}$$

where V_D is the diffusion potential, N_D the concentration of impurity, and ε_s the dielectric permeability of the semiconductor. When $\Phi B_O < \Phi B_S$, $\Delta\Phi_B$ is determined by the following formula:

$$\Delta\Phi_B = \Delta\Phi_{BO} \pm \beta qV. \tag{5}$$

Thus current–voltage characteristic of non-uniform real Shottky diode is expressed in forward bias:

$$\begin{aligned} I_F &= AA^*T^2 \exp\left(-\frac{\Phi_{BO}+\Delta\Phi_{BO}+\beta qV}{kT}\right)\left[\exp\left(\frac{qV}{kT}\right)-1\right] \\ &= AA^*T^2 \exp\left(-\frac{\Phi_{BO}+\Delta\Phi_{BO}}{kT}\right)\left[\exp\left(\frac{qV}{nkT}\right)-\exp\left(-\frac{(n-1)\,qV}{nkT}\right)\right] \\ &\approx AA^*T^2 \exp\left(-\frac{\Phi_{BA}}{kT}\right)\exp\left(\frac{qV}{nkT}\right), \end{aligned} \tag{6}$$

where for the last equation we have assumed $qV \gg kT$, in the reverse bias

$$\begin{aligned} I_R &= AA^*T^2 \exp\left(-\frac{\Phi_{BO}+\Delta\Phi_{BO}-\beta qV}{kT}\right)\left[\exp\left(-\frac{qV}{kT}\right)-1\right] \\ &= AA^*T^2 \exp\left(-\frac{\Phi_{BO}+\Delta\Phi_{BO}}{kT}\right)\left[\exp\left(-\frac{(1-\beta)qV}{kT}\right)-\exp\left(\frac{\beta qV}{kT}\right)\right] \\ &\approx AA^*T^2 \exp\left(-\frac{\Phi_{BA}}{kT}\right)\exp\left(\frac{qV}{n_r kT}\right). \end{aligned} \tag{7}$$

Considering the effect of R_s, equation (6) can be written as

$$I_F = AA^*T^2 \exp\left(-\frac{\Phi_{BA}}{kT}\right)\exp\left(\frac{qV}{nkT}\right) = I_S \exp\left(\frac{q(V-IR_s)}{nkT}\right), \tag{8}$$

where

$$I_S = AA^*T^2 \exp\left(-\frac{\Phi_{BA}}{kT}\right), \tag{9}$$

I_s is the saturation current density, Φ_{BA} is the effective BH at zero bias, A^* is the effective Richardson constant and is equal to 8.16 $A/cm^2 \cdot K^2$ for n-type GaAs, with n being an ideality factor serving as a measure of conformity of the diode to pure thermionic emission.

The barrier height can be obtained from Eq. (9) as

$$\Phi_{BA} = kT \ln(SAT^2/I_s). \tag{10}$$

Equation (8) can be recast into Eqs. (11)–(13) using Cheung's method[24] to calculate the barrier height, ideality factor and series resistance by using

$$\frac{dV}{d\ln(I)} = n\frac{kT}{q} + IR_s, \tag{11}$$

$$H(I) = V - n\frac{kT}{q}\ln\left(\frac{I}{AA^*T^2}\right), \tag{12}$$

$$H(I) = IR_s + n\Phi_{BA}. \tag{13}$$

Equations (11) and (12) should give a straight line each, thus, a plot of $dV/d(\ln I)$ vs. I will give R_s as the slope and $n(kT/q)$ as the y axis intercept. The ideality factor and the resistance are determined from the intercept and slope of Eq. (11). The barrier height may be calculated from Eq. (13) using the obtained n value.

5. Results

Figures 5 shows the dependences of diode ideality factor (n) and barrier height on diode diameter with and without R_s effects, and the dependence of R_s on diode diameter.

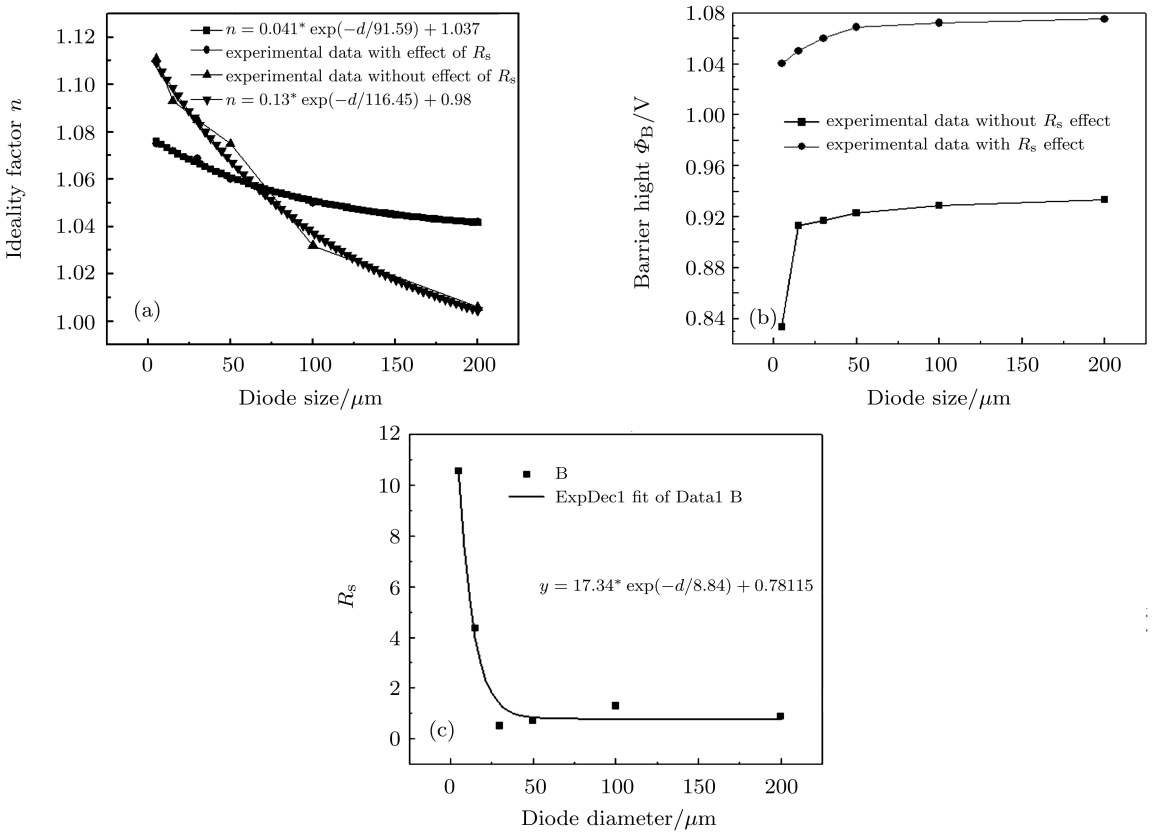


Fig. 5. Dependences of diode ideality factor (a), barrier height (b), diode resistance (c) on diode diameter.

The value of the ideality factor (n) varies from 1.11 to 1.006, and the barrier height (Φ_B) varies from 0. 833 to 0.933 V.

With the diode diameter increasing, the ideality factor (n) decreases (Fig. 5(a)), barrier heights (Φ_B) increase (Fig. 5(b)), and diode resistance R_s decreases. The figures show that these dependencies are nonlinear, which are in good agreement with the earlier reported results.[20,22]

From Fig. 5(b), we have $\Phi_{BA} = 0.926 -$

$0.238\exp(-d/5)$, and substituting this value into Eq. (9) yields a relation between I_s and diode diameter: the I_s first decreases by increasing the diode diameters and then it increases. The values of I_s for different diode diameters are plotted in Fig. 6. With the diode diameter increasing, the I_s value first decreases till $d = 15$ μm then it increases with diode diameter increasing (see the inset of Fig. 6).

Figure 7(a) shows the atomic force microscopic (AFM) image of the deposited Au, revealing that we have structural Au atoms on GaAs; the Au atoms are deposited on substrate homogenously. Figure 7(b) displays the phase image of the Au. Figure 7(c) exhibits the variation of the potential across the Au surfaces (marked as rectangular box in Fig. 7(b)) with a Gaussian fit. This figure shows that the potential distribution is Gaussian.

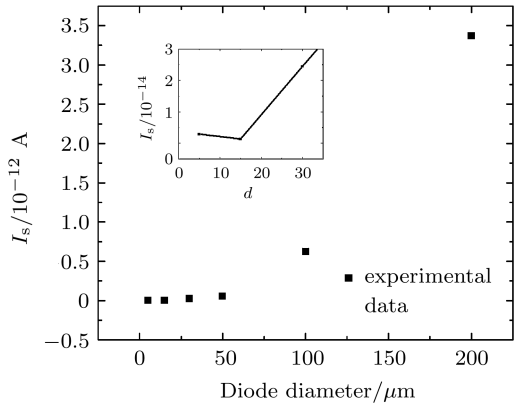


Fig. 6. Diameter dependence of saturation current, showing that with the increase of the diode diameter, I_s value first decreases till $d = 15$ μm then it increases with the increase of diode diameters (see the inset).

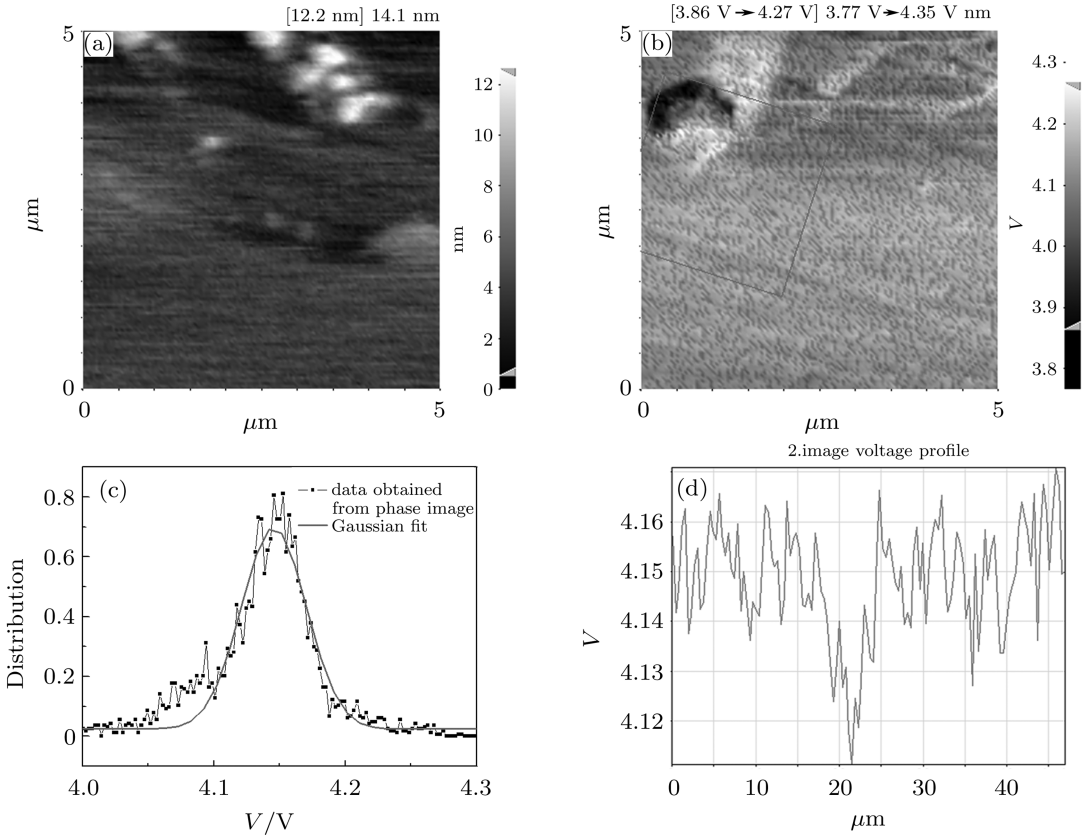


Fig. 7. Atomic force microscopic (AFM) image of the deposited Au on GaAs (a), the phase image of the Au (b), variation of the potential across the Au surfaces (marked as rectangular box in Fig. 7(b)) with a Gaussian fit (c), and the variation of potential in a submicron range (d), implying that we have patches in this area.

As seen from Fig. 7(d), the variation of potential is in a submicron range, implying that we have patches in this area. The formation of patches with various patch sizes ranging from approximately 100 nm to 200 nm can be the main source of various values of BH.

The patches indicate that we have parallel micro-and nanocontacts SD and the measurements of the operating parameters of SD, presented on Fig. 5, are determined by heterogeneity of interface of contacts. Apparently

from Fig. 5(b) between an operating barrier height ($\Phi_{\rm BA}$) of SD and its maximum distance (x) from interface, there is a certain correlation.

Dimensional dependences of the barrier height and the ideality factor of SD are determined by the change of the contribution of a peripheral current in SD with the diameter of contact increasing, and the increase in diameter of SD reduces the contribution of a peripheral current which causes an increase in the barrier height and a reduction of the ideality factor with the increase of diameter.

6. Conclusion

In the manufacturing process and after chemical processes by the immediate and careful transferring of diodes to the coating system, high quality Schottky diodes are produced where their reverse leakage current is found to be extremely low, thereby assuring a high quality rectifying behaviour. We find an increasing saturation current, decreasing BH and increasing ideality factor with diode diameter increasing, and a linear relationship between ideality factor (n) and BH. Investigation of electrical characteristics of the 5–200 μm diodes shows that by increasing the dimension, the potential barrier $\Phi_{\rm B}$ decreases so that it reaches 0.833 V for 5 μm and 0.933 V for 200 μm. With the diode diameter increasing, the ideality factor n decreases and reaches 1.006 in 200 μm diode and 1.11 in 5 μm diode. This shows that the diodes reach the ideality factor of one, whenever the dimension of the diode increases. Any real SD possesses non-uniform height of a barrier potential along a contact surface because the surface is of at least polycrystalline structure of metal. The topology of a surface of a thin metal film shows by atomic force microscope (AFM) that there is a granular structure with the sizes of approximately 100–200 nanometers. It means that Au/n type GaAs SD consists of parallel connected micro- and nano-contact diodes with the sizes of approximately 100–200 nm. Therefore in this work the presented measurement results, characteristics and parameters of SD well explain the heterogeneity of contact interface.

References

[1] Sonmezoglu S, Bayansal F, Guven Cankaya and Gaziosmanpasa 2010 *Physica* B **405** 287

[2] Abdul Manaf Hashim, Seiya Kasai and Hideki Hasegawa 2008 *Superlattices and Microstructures* **44** 754

[3] Mamedov R K 2003 *Contacts Metal–Semiconductor with Electrical Spots Field* (Baku: BSU) p. 231

[4] Semendy F, Singh S, Litz M, Wijewarnasuriya P, Blaine K and Dhar N 2010 *Solid-State Electronics* **54** 1

[5] Alperovich V L, Tereshchenko O E, Rudaya N S, Sheglov D V, Latyshev A V and Terekhov A S 2004 *Appl. Surf. Sci.* **235** 249

[6] Mehmet Ali Ebeoglu 2008 *Physica* B **403** 61

[7] Karatas S and Turut A 2006 *Physica* B **381** 199

[8] Zhang D H 1999 *Mater. Sci. Eng.* B **60** 189

[9] Keiji Maeda 2006 *Appl. Surf. Sci.* **252** 5659

[10] Schottky W 1938 *Naturwissenchaften* **26** 843

[11] Nakamura M, Yanagisawa H, Kuratani S, Iizuka M and Kudo K 2003 *Thin Solid Films* **438–439** 360

[12] Bardeen J 1947 *Phys. Rev.* **71** 717

[13] Song Y P, Van Meirhaeghe R L, Lauere W H and Cardon F 1986 *Solid-State Electron.* **29** 633

[14] Tung T 1992 *Phys. Rev.* B **45** 13509

[15] Sullivan J P, Tung R T, Pinto M R and Graham W R 1991 *J. Appl. Phys.* **70** 7403

[16] Tung R T 2001 *Mater. Sci. Eng.* **35** 1

[17] Tung R T 1993 *Contacts to Semiconductors* ed. Brilson L J (New Jersey: Noyes Publishers)

[18] Werner J H and Guttler H H 1991 *J. Appl. Phys.* **69** 1522

[19] Biber M, Cakar M and Turut A 2001 *J. Mater. Sci. Mater. Electron.* **12** 575

[20] Monch W 1988 *Phys. Rev.* B **37** 7129

[21] Monch W 1999 *J. Vac. Sci. Technol.* B **17** 1867

[22] Schmitsdorf R F, Kampen T U and Monch W 1997 *J. Vac. Sci. Technol.* B **15** 1221

[23] Savas Sonmezoglu, Sevilay Senkul, Recep Tas, Guven Cankaya and Muzaffer Can 2010 *Solid State Sciences*, in Press online 10 February 2010

[24] Detavernier C, Van Meirhaeghe R L, Donaton R, Maex K and Cardon F 1998 *J. Appl. Phys.* **84** 3226

[25] Somenath Roy, Chacko Jacob and Sukumar Basu 2004 *Solid State Sciences* **6** 377

[26] Yao Z, Postma H W C, Balents L and Dekker C 1999 *Nature* (London) **402** 273

[27] Cui Y and Lieber C M 2001 *Science* **291** 851

[28] Biswajit Ghosh, Madhumita Das, Pushan Banerjee and Subrata Das 2009 *Solid State Sci.* **11** 461

[29] Hasunuma R, Komeda T and Tokumoto H 1998 *Appl. Surf. Sci.* **130–132** 84

[30] Bell L D and Kaiser W J 1988 *Phys. Rev. Lett.* **61** 2368

[31] Tivarus C, Pelz J P, Hudait M K and Ringel S A 2005 *Appl. Phys. Lett.* **87** 182105

[32] Giannazzo F, Roccaforte F and Raineri V 2007 *Microelectronic Engineering* **84** 450

[33] Hasegawa H, Sato T and Kasai S 2000 *Appl. Surf. Sci.* **166** 92